Fuel 301 (2021) 121028

Contents lists available at ScienceDirect

Fuel

journal homepage: www.elsevier.com/locate/fuel

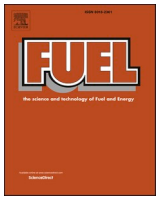

Full Length Article

Towards transportation fuel production from food waste: Potential of biocrude oil distillates for gasoline, diesel, and jet fuel

Jamison Watson [a], Buchun Si [b], Zixin Wang [a], Tengfei Wang [c], Amanda Valentine [a], Yuanhui Zhang [a,*]

[a] Department of Agricultural & Biological Engineering, University of Illinois at Urbana-Champaign, Urbana, IL 61801, USA
[b] Laboratory of Environment-Enhancing Energy (E2E), Key Laboratory of Agricultural Engineering in Structure and Environment, Ministry of Agriculture, College of Water Resources and Civil Engineering, China Agricultural University, Beijing 100083, China
[c] Faculty of Geosciences and Environmental Engineering, Southwest Jiaotong University, Chengdu 611756, China

ARTICLE INFO

Keywords:
Distillation
Transportation fuels
Hydrothermal liquefaction
Blendstock
Food waste

ABSTRACT

Biocrude oil from hydrothermal liquefaction (HTL) demonstrates promise as a supplement to the transportation fuel supply. However, its poor chemical (heteroatom content, energy content), physical (viscosity, density), and thermal (boiling point distribution, cetane value, cold-flow properties) characteristics limit commercial application. This study investigated the potential for the biocrude oil distillates derived from the mobile, pilot-scale HTL conversion of food waste to serve as a transportation fuel (gasoline, diesel, jet fuel) blendstock. Distillation increased the H:C (4.2–13.7%), decreased the O:C (5.5–93.5%), decreased the N:C (6.0–39.0%), and augmented the HHV (4.1–21.3%) compared to the biocrude oil, leading to values of 1.97, 0.003, 0.004, and 52.0 MJ•kg^{-1}, respectively. These values were similar to the H:C (1.65, 1.94, 2.02), O:C (0.02, ~0, ~0), N:C (0.0002, 0.002, 0.002), and HHV (50.0, 53.1, 53.4 MJ•kg^{-1}) values of gasoline, diesel, and Jet A fuels, respectively. With respect to the physical properties, distillation decreased the density (23.8–30.5%) and viscosity (99.5–99.9%), while the acidity either increased or decreased depending on the distillation temperature. Despite the benefits of distillation, blending is still required due to the poor N:C, viscosity, and acidity of the distillates. Theoretical blending calculations determined that blending with Jet A was the most favorable blendstock, amounting to deviations of 63.3–316.6% with the Jet A fuel when the distillate proportion ranged from 10 to 50%.

1. Introduction

The accumulation and mitigation of food waste has become an increasing point of interest for developing and developed nations alike. The U.S. Environmental Protection Agency estimates that 31% of the overall food supply is wasted, and approximately 94% of the food that is thrown away ends up in either landfills or incineration facilities [1,2]. These treatment methods suffer from a variety of drawbacks. Landfilling produces a leachate that necessitates dilution with large volumes of water to reach discharge standards [3]. A previous study noted that diverting food waste away from landfills could reduce environmental methane emissions by 9% while only leading to a 1% decline in energy production potential due to the inefficiency of harvesting methane [4]. As for incineration, due to the high moisture content of food waste, this processing technique is energy intensive, and it can release toxic air emissions and concentrated inorganic waste [5]. Thus, new techniques need to be explored that can utilize food waste to produce value-added products with minimal deleterious environmental impacts.

Hydrothermal liquefaction (HTL) is a thermochemical conversion process that converts high moisture feedstocks into biocrude oil and other value-added products. Typically, HTL is conducted in batch-type reactors (10–100 mL) at temperature and pressure conditions below or near the critical point of water (374 °C, 22 MPa) [6–8]. Previous studies have documented the successful batch conversion of food waste. Chen et al. demonstrated that biocrude oil derived from food waste exhibited a low ignition temperature, low burnout temperature, and a high combustibility index. This signified that biocrude oil derived from food waste was more combustible compared to biocrude oil derived from other feedstocks [9]. It should be noted that the biodegradability of food waste makes anaerobic digestion a formidable challenger to HTL treatment technology. Previous studies demonstrated large methane yields (0.1–0.9 m^3•(kg volatile solids)$^{-1}$) from the conversion of food waste.

* Corresponding author.
E-mail address: yzhang1@illinois.edu (Y. Zhang).

https://doi.org/10.1016/j.fuel.2021.121028
Received 6 March 2021; Received in revised form 4 May 2021; Accepted 8 May 2021
Available online 25 May 2021

However, the high content of protein and lipids in food waste can lead to inhibitory levels of ammonia and long chain fatty acids, cause foaming due to surface active materials or surfactants, and limit the system stability and economic viability of this treatment measure [10]. In addition, although the process energy input of HTL and upgrading (3.2 MJ•kg^{-1}) for the conversion of food waste was greater than anaerobic digestion (0.7 MJ•kg^{-1}), the energy recovery ratio was higher (HTL and upgrading: 0.8, anaerobic digestion: 0.1–0.6), and the emissions were similar (HTL and upgrading: 0.2 kg CO_2•kg^{-1}, anaerobic digestion: 0.1 kg CO_2•kg^{-1}) [11]. A previous study combining HTL and anaerobic digestion systems to develop a power-to-gas framework for the valorization of waste noted that from a techno-economic vantage point, anaerobic digestion accounted for a lower capital and operating cost ($255 million and $21 million•year^{-1}, respectively) than HTL ($484 million and $80 million•year^{-1}, respectively) [12]. However, the market for providing a renewable source of sustainable aviation fuels (SAF) via thermochemical conversion of food waste brightens the economic prospects of HTL technology relative to anaerobic digestion [13]. Despite the potential of HTL technology, several drivers still limit the fuel quality and upscale potential of this processing technology.

Aierzhati et al. demonstrated that the conversion of food waste model compounds led to a variability in the biocrude oil yield ranging from 2 to 79%, a heating value ranging from 32.7 to 40.4 MJ•kg^{-1}, and an energy recovery ranging from 17.2 to 75.1%. However, the content of oxygen and nitrogen still remained very high, amounting to 11.6–17.1 wt% and 0.2–8.7 wt%, respectively [14]. In addition to problems associated with oxygen- and nitrogen-containing derivatives, the success of food waste thermochemical conversion is limited to batch processing, and very few studies have achieved the conversion of food waste at the pilot-scale [15]. Thus, despite the inherent benefits of HTL conversion, the high heteroatom content and lack of scalability still need to be addressed before biocrude oil derived from HTL can achieve its commercial potential.

Distillation can isolate heteroatom-containing compounds. Pederson et al. determined that distillation separated complex chemical moieties into smaller groups that contain similar chemical structures. Furthermore, Pederson et al. found that light oxygenates distilled out into the lighter fractions, leading to ketones and other non-aromatic oxygenates being segregated to fractions with a boiling point below 250 °C [16]. Hoffman et al. found that fractional distillation caused the carbon content in biocrude oil derived from hardwood to increase from 83.9 to 88.2 wt%, the nitrogen content to decrease from 0.4 wt% to an undetectable level, and the oxygen content to decrease from 5.3 to 0.6 wt% [17]. Taghipour et al. also reported that fractional distillation influenced the physical properties of light and heavy biocrude oil distillates. It was concluded that fractional distillation decreased the viscosity by approximately 80% and 15% in the lightest and heaviest distillate fraction, respectively. Moreover, the density decreased in the lightest fraction by about 15%, and the density increased in the heaviest fraction by approximately 3% [18]. Despite the incorporation of fractional distillation to augment the physical and chemical properties of biocrude oil derived from HTL, no previous studies have directly compared the composition and properties of biocrude oil distillates to convention fuels (gasoline, diesel, and jet fuel) to better understand the future potential of combined HTL and upgrading technology to achieve a blendstock that can be sold on the market.

This study aims to systematically assess various physical, chemical, and thermal properties of the distillate fractions derived from the pilot-scale HTL conversion of food waste and assess the potential for biocrude oil distillates to be utilized as a blendstock (mixture of traditional fuels with HTL-derived fuel). The goals of this study are threefold: (1) Isolate compounds into groups of distillates using batch-scale distillation; (2) Investigate the physical, chemical, and thermal changes caused by distillation using instrumental and empirical methodology; (3) Compare and contrast groups of biocrude oil distillates with conventional fuel sources (gasoline, diesel, jet fuel) to determine the applicability of the different fractions towards transportation fuel production and assess blending potential.

2. Materials and methods

2.1. Feedstock and materials

The food waste feedstock was collected from a food processing plant in Champaign, IL. Upon collection, the food waste sample was homogenized using a commercial blender and mesh sieve with a wire spacing of approximately 5 mm (No. 4 mesh) to ensure a uniform particle size distribution and avoid clogging the reactor. Samples were stored in a fridge (4 °C) until experiments were conducted.

Unleaded gasoline was obtained from a local gas station in Champaign, IL. Off-road diesel (untaxed diesel, dyed diesel) was obtained from a local gas station in Champaign, IL. Jet A fuel was obtained from Willard Airport at the University of Illinois at Urbana-Champaign (Savoy, IL). The characteristics of the biocrude oil and base fuels are presented in Table 1.

2.2. Pilot-scale hydrothermal liquefaction

Pilot-scale HTL experiments were conducted in a continuous 30 L plug flow reactor (Snapshot Energy, LLC; Champaign, IL) [19,20]. Pictures and a representative piping and instrumentation design of the mobile, pilot-scale HTL system are provided in the Supplementary materials (Fig. S1, Fig. S2). HTL reactions were conducted at an average temperature of 280 °C, an average pressure of 10 MPa, and an average residence time of 60 min. The feedstock flow rate was maintained at 0.5 L•min^{-1}. The reactor system was composed of Schedule 40 stainless steel pipe with an inner pipe diameter of 1.9 cm. Nitrogen was then used to pressurize the system to prevent water from boiling. The feedstock was first pumped through the system using a diaphragm pump (Milton Roy high pressure pump; model MCHBG1-8FPEODM1SEST11NN22) with a check valve on both the inlet and outlet. A pulsation dampener charged with nitrogen was incorporated to absorb the impact of the pump stroke and lower the intensity delivered to the reactor. Subsequently, the feedstock was pre-heated by entering the cold side of the heat exchanger until it reached the main reactor inlet. Upon entering the reactor core, the feedstock was heated to the reaction temperature by semi-circular heaters connected in a ring. The converted product then left the reactor and entered the hot end of the heat exchanger where it was cooled to below 100 °C. Finally, the HTL product was pumped to the back pressure regulator and released into product collection tanks which was controlled by a reference pressure regulator and a metal diaphragm. The biocrude oil naturally phase separated from the aqueous phase. Therefore, the products were isolated by decanting without the incorporation of extraction solvents. A detailed and comprehensive description of the mobile, pilot-scale HTL system is available in the Supplementary materials.

2.3. Distillation

Distillation was conducted by adapting methods in previous reports [11,21]. Distillation experiments were conducted under atmospheric pressures. The experimental setup for atmospheric pressure distillation is presented in Fig. 1**A**. An additional diagram of the distillation unit is provided in the Supplementary materials (Fig. S3). Each distillation experiment involved loading biocrude oil into a 500 mL round-bottom flask. Approximately 20 g of 5 mm diameter glass beads (Fischer Scientific, Catalog Number: 11–312-10C) were added to the flask to facilitate mixing and allow the liquid to boil more calmly, thereby preventing the oil from violently leaving the flask and entering the fractional distillation column. Glass wool was wrapped around the flask and the column to reduce heat loss. A J-type thermocouple with a stainless-steel sheath was inserted into the top of the column to measure

Table 1
Elemental characteristics of the biocrude oil and base fuels.

Sample	Carbon[a]	Hydrogen[a]	Nitrogen[a]	Oxygen[a,b]	HHV (MJ•kg^{-1})	H:C[c]	O:C[c]	N:C[c]
Biocrude Oil	76.60 ± 0.05	10.99 ± 0.24	0.62 ± 0.02	11.81 ± 0.16	42.85 ± 0.35	1.74 ± 0.02	0.12 ± 0.01	0.0067 ± 0.0002
Gasoline	85.80 ± 0.14	11.66 ± 0.31	0.03 ± 0.01	2.53 ± 0.44	49.98 ± 0.56	1.65 ± 0.02	0.020 ± 0.002	0.00022 ± 0.00003
Diesel	86.67 ± 0.01	14.02 ± 0.01	0.24 ± 0.01	~0[d]	53.13 ± 0.01	1.94 ± 0.01	~0[d]	0.0023 ± 0.0001
Jet A	85.87 ± 0.12	14.45 ± 0.03	0.23 ± 0.01	~0[d]	53.43 ± 0.01	2.02 ± 0.01	~0[d]	0.0023 ± 0.0001

[a] Value determined based on dry weight percentage (wt.%).
[b] Calculated by difference.
[c] Value calculated on a molar basis.
[d] Value below detection limit of element analyzer; therefore, value was estimated at approximately 0 wt%.

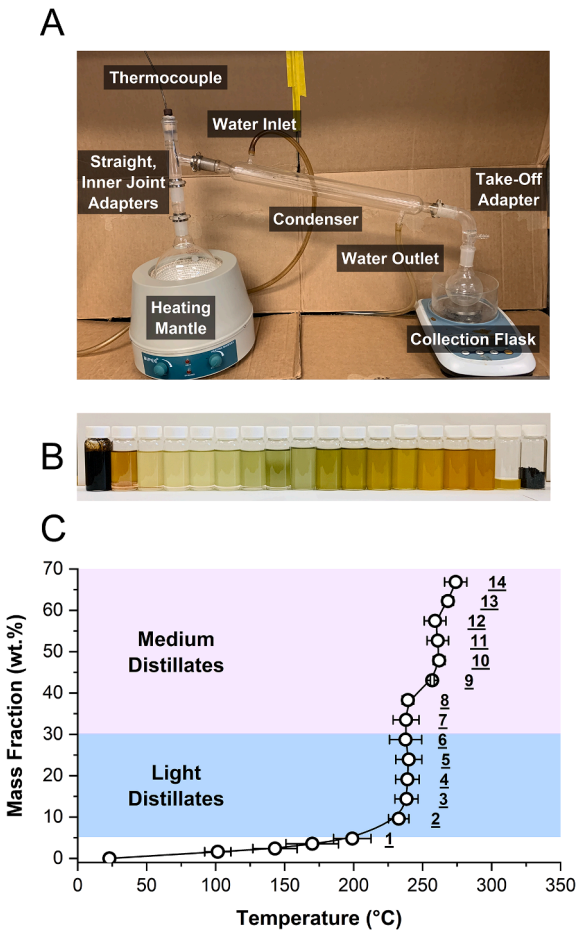

Fig. 1. Biocrude oil distillation experimental setup (A). Picture of the biocrude oil (left), 14 distillate groups (middle), and distillate residue (right) (B). Distillation mass recovery curve with respect to temperature (C). The points represent the finished elution of the given group. Four points were documented before the completion of the first group to ensure consistent heating and uniform elution over time.

the temperature of the vapor leaving the flask and entering the condenser. The flask was then heated with a 1,000 mL analog magnetic stirrer heating mantle (BIPEE, Model Number: 98–2-B-1000). The heating rate was set at approximately 2.5 °C•min^{-1} to ensure adequate separation of the different distillate fractions.

Regarding the specific equipment utilized for the distillation unit in this study, a 30 mm straight connecting adapter with a joint size of 20/40 (Chemglass, CG-1007–01) was affixed to the round bottom flask. An additional 24/40 joint size adapter (Chemglass, CG-1022–01) with a side inner joint angle of 75° that connected the straight adapter to connect the round bottom flask to the condenser unit. Upon volatilization of the biocrude oil, the vapor distillate passed through the adapters and into a 200 mm water-jacketed condenser unit (Chemglass, CG-1230–09) which was cooled by circulating tap water (25 °C) through the condenser unit. The condensed material was then dripped into a 20 mL graduated cylinder by passing through a take-off adapter (Chemglass, CG-1050–01) bent at a 105° angle. Approximately 15 g of distillate material was collected per distillate group. The remaining material in the flask after fractional distillation concluded was the distillate residue. In total, 14 groups of distillates were obtained in sequence (Fig. 1**B**). All physical, chemical, and thermal properties of the distillates were measured within one week after being recovered at avoid any changes associated with instability.

2.4. Analysis of products

Proximate analysis of the HTL food waste feedstock was conducted by Midwest Laboratories. The crude protein (AOAC 990.03) crude fat (AOAC 945.16), lignin (AOAC 973.18), and ash (AOAC 942.05) were experimentally determined according to methods established by the Association of Official Agricultural Chemists (AOAC) [11]. The acid detergent fiber and neutral detergent fiber were determined according to Ankom Technology standard methodology (A2000). The proximate and ultimate analyses of the food waste feedstock are presented in the Supplementary materials (Table S1).

Elemental analysis of the oil and solid product was conducted utilizing a CE440 element analyzer (Exeter Analytical; North Chelmsford, MA). The oxygen content was calculated by difference. The higher heating value (HHV) of the biocrude oil samples was calculated based on Dulong's formula [22].

The chemical characterization of the biocrude oil samples was conducted via gas chromatography mass spectrometry (GC–MS) (Agilent Technologies; Santa Clara, CA). A 2 µl sample was injected in split mode into a system comprised of three components: an Agilent 6890 chromatograph, an Agilent 5973 mass detector, and an Agilent 7683B autosampler. A 60 m ZB-5MS column was employed for analyte separation with a nominal diameter of 0.32 mm and a film thickness of 0.25 µm. The injection temperature was set at 250 °C, and the oven temperature was initially set at 70 °C and then ramped at 5 °C•min^{-1} to 300 °C. The source temperature was set at 230 °C, and the electron ionization voltage was set at 70 eV. Spectra were scanned from 30 to 800 *m/z*, and the characterization of individual peaks were determined by comparing mass fragmentation patterns of the peak to the NIST (NIST08) database. All GC–MS data was normalized by the internal standard: 0.5 uM pentadecanoic acid. The detailed analytical procedure for GC–MS was previously described in the literature [23].

The mass distribution and average molecular weight of the chemical components in the biocrude oil were analyzed via matrix-assisted laser desorption/ionization time of flight mass spectrometry (MALDI-TOF-MS). MALDI-TOF mass spectra measurements were conducted using a Bruker Autoflex Speed LRF instrument (Bruker Scientific Instruments; Germany) with dual microchannel plate detectors for both linear and reflectron modes. In accordance with the manufacturer's instructions, MALDI-TOF was used with Flexcontrol software 3.0 (Bruker Daltonics) for the automatic acquisition of mass spectra in the reflectron positive

mode within the range 150 to 1500 Da. The acceleration voltage was + 19 kV, and ions were measured in reflectron mode. Trans-2-[3-(4-*tert*-Butylphenyl)-2-methyl-2-propenylidene]malononitrile (DCTB) was used as the matrix reagent. Samples used for MALDI-TOF-MS analysis involved the addition of l μl of liquid product and 10 μl of the matrix solution, then 1 μl of this mixture (10 mg•mL^{-1}) was placed on the MALDI target plate for subsequent testing before being mixed with the matrix.

Functional group characterization was determined via Fourier transform infrared spectroscopy (FTIR). Sample spectra were obtained using a Thermo Nicolet Nexus 670 spectrophotometer in transmission mode under atmospheric conditions. Prior to sample analysis, the spectra were normalized and calibrated in order to minimize deviations associated with background measurements. A smart multi-bounce combination kit for liquids and solids (ThermoFischer Scientific, Catalog Number: 00282XX) was incorporated for obtaining the spectra of the sample with an IR source and KBr as the beamsplitter. The analyzed spectral range was 800–4000 cm^{-1}. All samples were collected with a resolution of 2 cm^{-1} and 40 total scans. The detailed analytical procedure for GC–MS was previously described in the literature.

Thermal properties and distillate temperature ranges were conducted via thermogravimetric analysis (TGA). Approximately 10–20 mg of sample was placed in a quartz crucible. The crucible was the transferred to a platinum pan and delivered to the Cahn TherMax 500 TGA system. Samples were heated from room temperature up to 650 °C at a ramp temperature of 10 °C•min^{-1} while under a nitrogen flow rate of 22 mL•min^{-1}. The calculated cetane index (CCI) was determined using a standard test method incorporated a four variable equation (ASTM D4737-10) [24]. The calculated flash point (CCF) was determined using a standard method involving recovery temperatures (ASTM D7215-16) [25]. The recovery temperatures were determined via TGA. It should be noted that since the CCI equation does not consider the addition of cetane improvement additives, the CCI is equal or less than the true cetane number of the fuel. A high CCI (maximum 100) indicates that the auto-ignition characteristics of the tested fuel are like that of a reference fuel (cetane). Thus, the higher the value, the better the auto-ignition characteristics. The CCF is an important fuel characteristic because it prevents storage and transportation of fuels. Thus, keeping storage temperature below the CCF ensures that the mixture of air and fuel vapors remains below the flammability limits [26].

The acidity (total acid number) of the samples in this study were determined via color-indicator titration according to standard methods (ASTM D974-12) [27]. In short, reagent grade p-Naphtholbenzein (Fischer Scientific, CAS: 145–50-6) was utilized as the indicator solution and placed in an Erlenmeyer flask. The oil sample was then dissolved in the indicator solution. KOH was then titrated into the indicator/sample solution using a 50 mL graduated buret in 0.1-mL subdivisions. When the end point was reached (determined via indicator color change from orange to green–brown), the amount of KOH added per gram oil was utilized to determine the total acid number. The kinematic viscosity of the oil samples was determined using a Cannon-Fenske routine viscometer at 20 °C according to standard methods (ASTM D446-12) [28]. Vacuum was used to draw the sample through the bulb of the viscometer to a point 5 mm above the timing mark. Subsequently, vacuum was released, and the sample could flow by gravity. The amount of time (to the nearest 0.1 s) required for the leading edge of the meniscus to pass from the first timing mark to the second timing mark on the viscometer was recorded, and the time in tandem with the approximated constant for calibration was used to determine the kinematic viscosity (mm^2•s^{-1}) of the sample. The density was determined using a 2-mL glass Gay-Lussac bottle with an outside diameter of 0.67 in (Cole-Palmer, EW-34580–40) [29].

3. Results & discussion

3.1. Distillation curves

The distillation curve is presented in Fig. 1**C**. The initial boiling point (IBP) of the biocrude oil using the distillation setup in this study was 84.0 °C. The IBP was defined as the average temperature at which the first drop of condensate was measured in the collection flask. This value was similar to the IBP of green jet fuel (104.3 °C), which was derived from the thermocatalytic cracking of crude palm oil [30]. The relatively low IBP could have been attributed to the presence of moisture and light oxygenates. The light naphtha distillate temperature region (<100 °C) only comprised 1.6% of the mass balance, which was identical to the results for the fractional distillation of oil derived from aspen wood liquefaction [16]. The final boiling point (FBP) of the biocrude oil using the distillation setup in this study was 274 °C. As shown in Fig. 1**C**, from the initial collection of the condensed distillate to ~ 200 °C, the temperature to mass fraction collected was nearly linear, accounting for only 4.8% of the total mass balance. Exceeding a temperature of ~ 233 °C led to a nearly vertical trend, with only slight deviations (±6.7 °C) in the average distillation temperature over this region. The reason for the stagnant temperature was because the energy associated with the temperature could not overcome the intermolecular forces holding these compounds together until these compounds were vaporized. This signified the presence of an abundance of compounds between the temperatures of 233–239 °C which accounted for a mass fraction of ~28.7%. A similar trend was observed at 257–273 °C, which accounted for 28.6% of the mass fraction. These trends could have been attributed to the presence of saturated and unsaturated fatty acid derivatives, which have boiling points within this temperature range.

Overall, 66.9% of the biocrude oil was recovered up to a maximum temperature of 274 °C, amounting to a distillate residue fraction of 13.0%. These values are in line with previous studies which found that distillation could extract 62–67%, 70–73%, and 61% of the total biocrude mass from the oil derived from HTL and pyroloysis of *Spirulina* sp., *Tetraselmis* sp., and rice husk, respectively [31,32]. However, it should be noted that 20.1% of the mass fraction was not recovered, which could have been attributed to insufficient cooling of the vapor leading to the escape of gas over the long fractional distillation time (~112 min). Vacuum distillation should be utilized in future studies to overcome thermal changes when distillation temperatures exceed 250–300 °C and therefore recover a greater amount of biocrude distillates. The detailed information regarding the fractional distillation temperature, mass fractions, elution times, and categorization of the 14 distillate fractions are presented in the Supplementary materials (Table S2).

Fig. S4 demonstrates the consistency of the fractional distillation process. There was a nearly linear relationship between the cumulative mass collection and the fractional distillation time, signifying a stable temperature ramp during the fractional distillation process and that thermal degradation could have been avoided. A previous study also noted the distillate volume fraction of biocrude oil derived from glycerol-assisted liquefaction of swine manure increased almost linearly from 10% to 90% as the temperature increased [33].

3.2. Elemental composition

Fig. 2 and Fig. S5 provide an illustration of the carbon, oxygen, nitrogen, hydrogen, and energy contents and balances of the fractional distillates. From the data presented in Fig. 2, fractional distillation was able to effectively recover the carbon and hydrogen within the distillate fractions, and the content of oxygen greatly reduced. The nitrogen content did not markedly decrease compared to the biocrude oil. The elemental content graphs bolster the idea from the mass recovery curve (Fig. 1**C**) that there is a demarcation between two groups of distillate fractions with similar properties (light distillates: 1–6; medium distillates: groups 7–14).

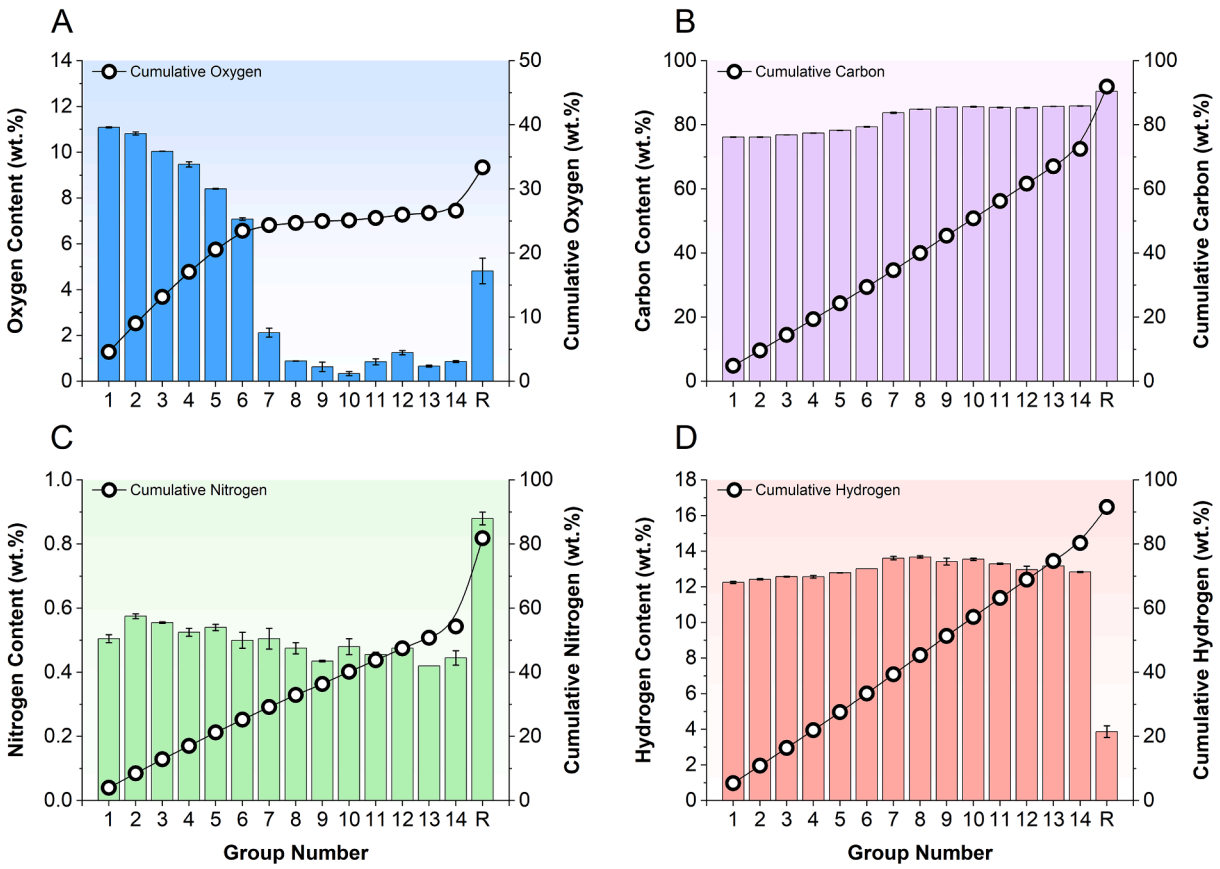

Fig. 2. Oxygen (A), carbon (B), nitrogen (C), and hydrogen (D) content of the biocrude oil distillates. R represents the distillation residue.

Regarding the oxygen content (Fig. 2**A**), the first distillate fraction (11.1%) had a very similar oxygen content as the original biocrude oil feedstock (11.8%); however, the oxygen content then decreased rapidly to 7.1% as the fractional distillation temperature increased to 239 °C (group 6). The high oxygen content in the first few groups could have been attributed to oxygen-containing low molecular weight moieties or moisture. A previous study noted that despite dewatering of oil, reaction water can be formed through condensation reactions at elevated temperatures and subsequently condense in the condenser unit and elute into the sample vials [34]. This also supports the reason for the low IBP of the biocrude oil. Thereafter, for subsequent groups (groups 7–14) the oxygen content was noticeably lower, amounting to oxygen contents ranging from 0.3 to 2.1%. It should be noted that approximately 66.6% of the total oxygen mass in the biocrude oil was not recovered, since only 6.8% of the mass was accounted for in the distillate residue (Fig. S2). This signifies that most of this element was lost through the escape of distillate gas. Volatilization of these compounds could have occurred. This could have been avoided by incorporating a longer condenser unit, a greater flow rate of cold water, or by employing a recirculation unit to maintain well-controlled cooling [35].

As for the carbon content, nearly all the carbon mass was recovered in either the distillate fractions or in the distillate residue (91.9%). The carbon content trends were the inverse of the oxygen content trends; however, the changes were not as drastic. The carbon content slowly increased from 76.2% to 79.4% as the fractional distillation temperature increased (group 1 and group 6, respectively). The carbon content then increased and remained relatively stable for groups 7–14, amounting to a total content ranging from 83.8 to 85.9%. Notably, the carbon content in the distillate residue was quite high, reaching a value of 90.4% (Table S3). This could signify that there could be many high molecular weight constituents (boiling point >274 °C) remaining in the distillate residue that could be further extracted by thermochemical hydrocracking.

Regarding the nitrogen content, distillation did not impact the content of nitrogen in the various distillates. Thus, the nitrogen compounds were evenly distributed amongst all the 14 distillate cuts despite the increase in the fractional distillation temperature. The nitrogen content ranged from 0.4 to 0.6% among all distillate samples. Notably, the nitrogen content was much higher in the distillate residue in comparison to the distillate fractions, amounting to up to 0.9% in the residue. In total, the nitrogen content only conservatively decreased in comparison to the nitrogen content of the biocrude oil (0.6%). The distillate residue accounted for 23.6% of the nitrogen distribution, while all distillate fractions collectively accounted for 54.3%. Thus, the composition of the distillate residue contained a variety of high molecular weight nitrogen-containing compounds.

Finally, the hydrogen content displayed a similar trend as the carbon content. The cumulative hydrogen content among the 14 distillates linearly increased as the distillation temperature increased. Furthermore, the distillate residue only had a minimal hydrogen content, account for a total distribution of 3.9%, which was drastically lower than the hydrogen content of the distillate fractions (12.3–13.7%). This signifies that the residue could be composed of unsaturated cyclic or acyclic hydrocarbons.

The elemental contents of the fractional distillates were used to create a Van-Krevelen diagram (Fig. 3). From the data presented in Fig. 3**A**, the light distillates (groups 1–6) had both a high O:C ratio and N:C ratio, amounting to 0.067–0.11 and 0.0054–0.0065, respectively. The values of the light distillates had properties that were more similar to the HTL biocrude oil; however, distillation led to a lower O:C (5.5–42.1%), N:C (6.0–21.6%), and an increased HHV (4.1–11.2%) compared to the biocrude oil for the light distillate fractions. However, an even more notable difference was observed for the medium distillates (groups 7–14). The change in the N:C (24.9–39.0%), O:C (83.5–97.5%),

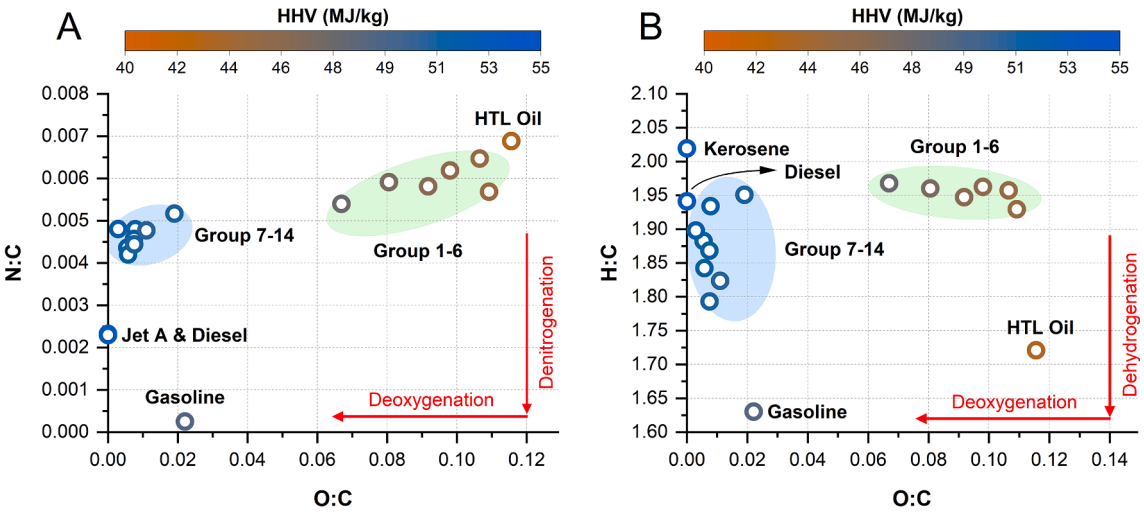

Fig. 3. Van Krevelen diagram of biocrude oil distillates and base fuels.

and HHV (18.9–21.3%) were even more apparent for the medium distillates, and the quality of the biocrude oil for these groups was more similar to conventional fuel sources (Jet A and gasoline). However, a significantly greater reduction in the N:C ratio is still needed in order to be comparable to all conventional fuel sources.

Fig. 3**B** demonstrates similar trends as previously discussed. Notably, the light distillates had a higher H:C ratio (1.9–2.0) in comparison to gasoline (1.6) and a comparable value to that of both diesel and Jet A (1.9–2.0). These results are similar to those presented in a previous study which demonstrated that low temperature distillates had a higher H:C (1.8–1.9) in comparison to the high temperature distillates (1.3–1.5) [36]. The data presented indicates that subsequent hydrotreating is needed for the high temperature distillates, and hydrodeoxygenation is needed for the low temperature distillates to achieve a Jet A or diesel product. Despite the low nitrogen content in the biocrude oil, additional denitrogenation is still needed for all distillates and is a limiting factor for the commercialization of biocrude oil.

3.3. Chemical characterization

Fig. 4 demonstrates the distribution of chemical compounds for the distillates and base fuels. From the distribution of chemicals, it is clear that the high H:C ratio in the light distillates was attributed to the presence of long-chain fatty acid derivatives (38.6–48.7%). For example, fatty acids such as hexadecanoic acid, pentadecanoic acid, and decanoic acid were prevalent in the light distillates, but they were only sparsely detected in the medium distillates. The increased presence of olefins in the medium distillates (36.7–42.1 wt%) also further verifies the reason for the decrease in the H:C ratio as the fractional distillation temperature increased. Thus, the primary chemical constituents that were impacted by fraction fractional distillation were carboxyl groups, compounds containing units of unsaturation, and hydrocarbons.

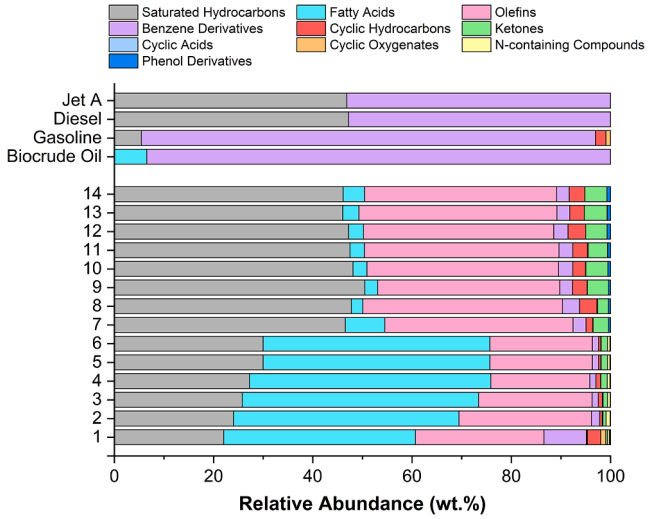

Fig. 4. GC–MS results for the biocrude oil distillates and base fuels.

With respect to the base fuels, benzene derivatives (toluene, ethylbenzene, xylene, etc.) accounted for a large fraction of the relative weight distribution (52.8–91.5%). It should be noted that the base fuel composition can vary widely because these fuels are a blend of several refinery streams [37]. Thus, the chemical composition and additives may differ from region-to-region. The high benzene derivative content can be attributed to the inclusion of additives to improve the cetane and octane number of the fuels [38,39]. Notably, the biocrude oil shared similarities with the gasoline fraction, but it contained fatty acids in lieu of saturated hydrocarbons. However, it should be noted that GC–MS only provides a qualitative distribution of compounds with boiling points below the GC–MS oven temperature (300 °C); thus, the gamut of chemical compounds present in the biocrude oil cannot be elucidated by GC–MS alone [40].

Regarding the olefins, Table S4 depicts the impact of distillation on the composition of the unsaturated hydrocarbon compounds. Notably, the distribution of decene, dodecene, and tridecene (C_{10}-C_{13} compounds) increased as the fractional distillation temperature increased. Conversely, the distribution of heptadecene and octadecene (C_{17}-C_{18} compounds) generally increased and then decreased as the fractional distillation temperature increased. In general, the diversity of olefins remained the same for both light and medium distillates, but the concentration of each species tended to increase transitioning from the light to medium distillates. The most abundant olefin (heptadecene) dominated between groups 2–4 (fractional distillation temperature range: 225–248 °C), accounting for 51.4–60.0% of the olefin fraction and 10.2–16.0% of the total biocrude oil fraction.

Table S5 demonstrates the impact of fractional distillation on fatty acid derivatives. From the data, the content of the fatty acid derivatives initially increased and then decreased substantially. Notably, fatty acids were concentrated in the light distillates, accounting for 38.6–48.7% of the total biocrude oil content. Decanoic acid, pentadecanoic acid, hexadecenoic acid, octadecanoic acid, and octadecenoic acid accounted for up to 73.2–84.7% of the fatty acid derivatives and occupied up to 28.3–41.2% of the total biocrude oil content. Considering the vast market for natural fatty acids, subsequent studies should be conducted

to isolate the fatty acid derivatives in the light distillate region. This can be done by conducting subsequent distillation experiments or sequential distillation with greater temperature control to better isolate the fatty acids from the other compounds in the distillate fractions. Column chromatography could also be another interesting method to isolate polar and non-polar compounds thereby isolating fatty acids from the bulk of the material [41]. Fatty acids are not beneficial for incineration, because they could lead to corrosion of the engine [21]. Thus, the light distillates need subsequent decarboxylation or neutralization to be directly applied as a transportation fuel. The fatty acid content decreased substantially from a maximum of 48.7% in group 4 to a minimum of 2.3% in group 8. Thus, subsequent studies should focus on isolating or converting the fatty acids depending on the end use case (chemicals or fuel).

Finally, regarding hydrocarbons (Table S6), the content increased as the fractional distillation temperature increased, accounting for a minimum of 22.1% in the light distillates and a maximum of 48.1% in the medium distillates. Thus, the medium distillates demonstrate great promise as serving as a hydrocarbon fuel source. Under the presumption that the olefin fraction is converted to saturated hydrocarbon through catalytic hydrogenation, the saturated hydrocarbons could represent between 84.5 and 88.0% of the total biocrude oil weight fraction. Subsequent model compound studies should be conducted to optimize the conversion of olefins to hydrocarbons. Since these fractions only demonstrate a minimal composition of other chemical species, it is likely that catalytic hydrogenation will not be impeded (sintering, coking, etc.).

The FTIR results help to bolster the findings provided by the GC–MS analysis (Fig. 5). There were a few primary changes in the FTIR curves as the fractional distillation temperature increased. First, the peak at ~1710 cm^{-1} greatly diminished as the fractional distillation temperature increased. Peaks at this wavenumber are generally associated with C = O stretching, which could be indicative of the presence of conjugated aldehydes/ketones [42]. This peak could be associated with the presence of fatty acid derivatives, which demonstrated that as the distillation temperature increased, the presence of these compounds diminished. This agrees with the GC–MS results. Another notable feature was the increased presence of the ~1450 cm^{-1} peak. This peak is typically associated with C–H bending, which could indicate the increased presence of saturated carbon compounds. This is significant because the base fuels all have a pronounced peak at ~1450 cm^{-1}.

The MALDI results demonstrate the weight distribution of compounds in the distillate fractions and base fuels (Fig. 6). From the data presented in Fig. 6**A**, as the distillation temperature increased, the average molecular weight decreased. Specifically, the molecular weight decreased from a maximum value of 503.5 Da to a minimum of 321.9 Da

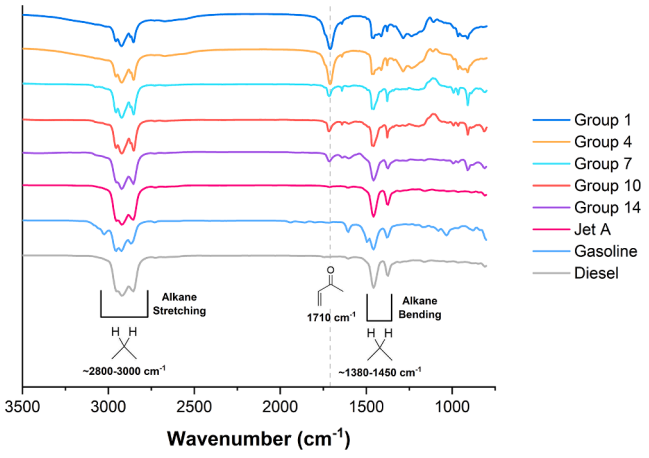

Fig. 5. FTIR spectra comparison between representative biocrude oil distillates (groups 1, 4, 7, 10, and 14) and base fuels.

as the distillation temperature increased. Thus, the low temperature distillates had an average molecular weight similar to biocrude oil (533.2 Da) and the high temperature distillates had an average molecular weight closer to the base fuels (247.5–278.2 Da). The polydispersity index is also presented in Fig. 6**A**. This value indicates the heterogeneity of the sizes of molecules in a mixture. A value of 1 signifies a perfectly homogeneous size distribution of molecules. As the distillation temperature increased, the polydispersity index decreased from 1.5 to 1.3, indicating a more homogeneous size distribution. Although distillation was able to enhance the homogeneity of the extracted compounds (light distillates: 1.5, medium distillates: 1.3–1.4) compared to the biocrude oil (1.6), but it was still not able to achieve a near-uniform distribution as presented in the base fuels (1.1–1.2).

From the results in Fig. 6**B**, the variety of weights was vast at the beginning of distillation, but the values slowly started to center around 200–400 Da as the distillation temperature increased. This data bolstered the GC–MS results which indicated the accumulation of saturated/unsaturated hydrocarbons and fatty acids with molecular weights that fall within this range (Table S4, Table S5, and Table S6). Specifically, for group 1, only 12.0% of the compounds had a molecular weight ranging from 200 to 300 Da. Thus, the accumulation of compounds >500 Da attributed to the higher molecular weight of the initial distillates and the accumulation of compounds in the 200–400 Da as the temperature increased lowered the average molecular weight.

3.4. Physical properties

Fig. 7 demonstrates the impact of distillation on the physical properties of the biocrude oil distillates. In general, the viscosity initially increased as the distillation temperature increased from 3.2 $mm^2 \bullet s^{-1}$ to a local maximum of 4.5 $mm^2 \bullet s^{-1}$. Thereafter, the viscosity decreased to a global minimum of 1.5 $mm^2 \bullet s^{-1}$ and then increased steadily. The change in the viscosity can be explained by the intermolecular forces governed by the composition of the distillates. The concentration of fatty acids in the initial distillation groups could have led to increased hydrogen bonding and dipole–dipole interactions, which could have increased resistance to flow. Subsequently, the depleted presence of intermolecular forces decreased the viscosity. Finally, as the distillation temperature increased, the relative concentration of saturated compounds and olefins increased, which could have enhanced London dispersion forces, resulting in a higher resistivity to flow in the last distillates. Another factor attributed to the change in the viscosity could be the change in the concentration of branched aliphatics, a change in the overall length of aliphatics, and fewer intermolecular reactions as the number of compounds in the distillates decreased [29]. The viscosity of the biocrude oil was 983.9 $mm^2 \bullet s^{-1}$, demonstrating that distillation significantly decreased the viscosity. In comparison to the base fuels, most low temperature and high temperature distillates had a similar viscosity to diesel (4.1 $mm^2 \bullet s^{-1}$). However, groups 6–9 had a viscosity much more similar to Jet A fuel (2.0 $mm^2 \bullet s^{-1}$). The high viscosity of groups 1–5 is supported by the MALDI results which demonstrated that a significant portion of the compounds had a molecular weight greater than 400 Da (31.2–51.4%).

Distillation temperature demonstrated an obvious effect on the acidity. The high acidity of the first 5–6 distillate groups was attributed to the presence of an abundance of fatty acid derivatives, which was supported by the GC–MS results. The acidity first increased from 150.0 up to 207.3 $mg \bullet g^{-1}$. Thereafter, the acidity content continued to fall and remain at a level ranging from 0.0 to 9.4 $mg \bullet g^{-1}$. Upon reaching a temperature of ~240 °C, all the fatty acids were distilled, thereby leading to the subsequent distillates having a substantially less acid content. The acidity of the base fuels ranged from 12.4 to 28.8 $mg \bullet g^{-1}$. Thus, the acidity of the first few groups needs to be substantially reduced to comply with fuel standards. This could be achieved through various upgrading processes, including hydrodeoxygenation, hydrodecarbonylation, esterification, or cracking reactions [11,43]. Fatty acid

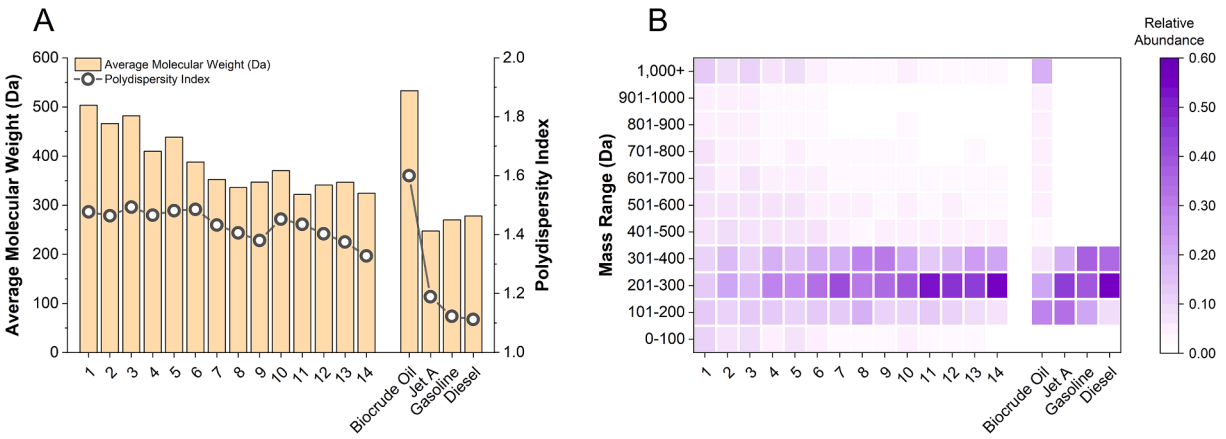

Fig. 6. Average molecular weight and polydispersity index of the distillates and base fuels (A). Relative abundance of distillates and base fuels at different weight distributions for the distillates and base fuels (B).

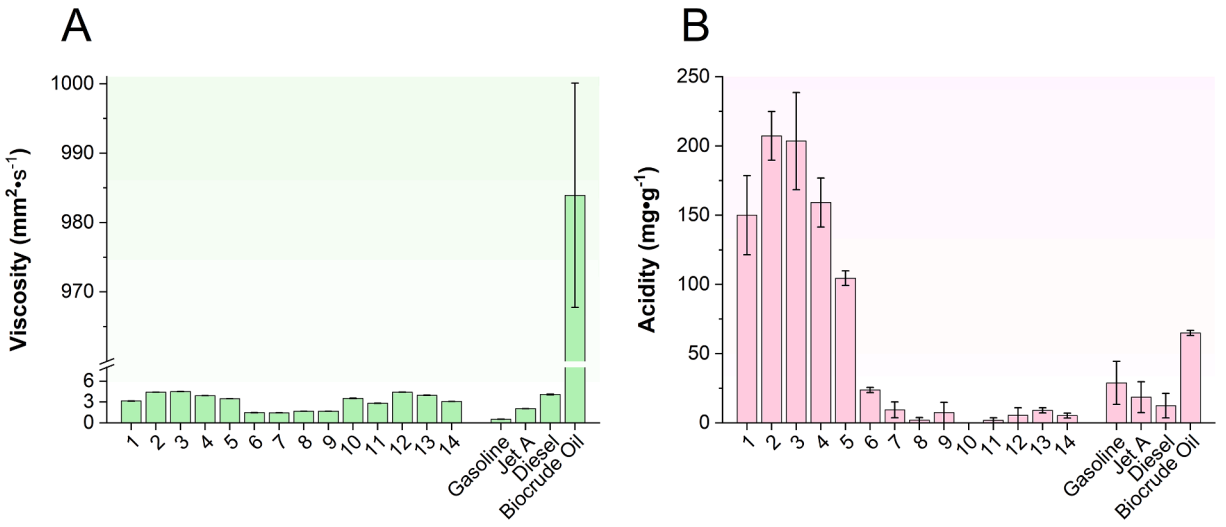

Fig. 7. The impact of distillation on the viscosity and acidity of the biocrude oil distillates and base fuels.

Table 2
Empirical calculation of thermal properties of distillates and base fuels based on thermogravimetric analysis.

Sample #	T_5 (°C)	T_{10} (°C)	T_{25} (°C)	T_{50} (°C)	T_{75} (°C)	T_{90} (°C)	CCI[a]	CFP (°C)[b]
1	69.81	91.79	133.14	170.28	198.17	225.75	23.63	−2.57
2	86.44	113.42	157.09	190.36	213.61	231.67	23.20	10.16
3	87.00	113.95	158.02	192.16	216.41	235.11	23.67	10.37
4	82.37	109.79	156.05	192.46	217.32	234.43	25.44	7.56
5	82.78	109.12	154.08	191.15	216.75	233.38	25.55	7.60
6	77.05	97.86	133.99	169.43	195.70	211.68	26.85	2.00
7	60.05	79.43	116.37	157.23	185.82	200.33	31.39	−8.81
8	72.26	93.59	132.67	172.71	199.36	212.85	43.14	−0.74
9	64.12	84.47	122.44	162.14	189.04	202.60	28.61	−5.68
10	94.88	123.45	171.10	209.28	232.76	245.16	37.36	15.75
11	79.00	106.08	153.04	197.16	244.98	239.24	36.51	5.41
12	98.74	131.31	185.90	232.31	260.45	274.75	41.15	19.76
13	92.84	123.48	176.89	229.23	262.47	278.81	39.43	15.24
14	84.15	110.32	158.36	209.21	245.18	263.89	29.88	8.32
Residue	236.86	264.84	497.63	–	–	–	–	115.61
Biocrude Oil	236.96	257.45	297.34	389.11	427.14	464.55	~0[c]	113.40
Gasoline	34.64	40.28	54.34	70.64	84.75	94.10	48.50	−28.93
Diesel	102.7	120.32	148.57	77.18	200.98	218.18	21.24	18.28
Jet A	81.16	95.67	118.39	140.92	159.63	170.77	18.95	2.95

[a] The calculated cetane index (CCI) was determined according to ASTM D4737-10.
[b] The calculated flash point (CFP) was determined according to ASTM D7215-16. The initial boiling point (IBP) of each distillate was assumed to be the temperature when 0.5% of the organic matter volatilized according to thermogravimetric results obtained via TGA.
[c] Value below limit for CCI equation. Value assumed to be 0.

derivatives are the reason for the high acidity of biocrude oil (64.9 mg•g^{-1}), and distillation could be an effective method to reduce acidity.

3.5. Thermal properties

TGA was incorporated to determine fuel properties based on the boiling point distribution and recovery temperatures. These techniques were adapted from empirical evidence derived from fuel property correlation assessments [44,45]. Table 2 presents the recovery temperatures, calculated cetane index (CCI), and calculated flash point (CFP) of the distillate fractions and base fuels. The recovery temperatures presented in the table are indicative of the temperature where a certain percentage of the fuel was volatilized. For example, a T_{10} value of 100 °C indicates that at 100 °C 10% of the fuel weight was volatilized. From the data presented in Table 2, the recovery temperature, CCI, and CFP all tended to oscillate as the fractional distillation temperature increased, first increasing slightly, decreasing, and then finally increasing to maximum values. The improved CCI could be attributed to the separation of the distillate residue, which contained chemical compounds recalcitrant to vaporization, which can be observed due to the high T_{10} and T_{25} values of 264.8 °C and 497.6 °C, respectively. Similar to the GC–MS results, there was a clear demarcation between the light and medium distillates. The CCI of the former was 23.2–26.9 while the range of the latter was 29.9–43.1. All distillates showed marked increases in the CCI compared to biocrude oil. However, it should be noted that the light distillates had a similar CCI with that of diesel and Jet A, whereas the medium distillates had a similar CCI to gasoline. Despite the relatively lower values of CCI for the light distillates, cetane enhancers (nitrates, nitroalkanes, etc.) can be added to achieve the cetane number of gasoline fuel, which is a common industry practice [46]. As for the CFP, both light and medium distillates demonstrated significant decreases (-2.6–19.8 °C) in comparison to biocrude oil (113.4 °C). This could be directly attributed to the separation of the distillate residue, which was composed of unsaturated, high molecular weight, nitrogen- and oxygen-containing compounds with a CFP value of 115.6 °C.

3.6. Fuel quality correlation and blending potential

Fig. 8 illustrates a correlation plot demonstrating the relationship among the different fractional distillation variables. The strength of the correlation is indicated by the size and color of the circles. Notably, the distillation temperature was positively ($R^2 \geq 0.7$) correlated with the carbon content and energy content. In addition, fractional distillation temperature was strongly negatively correlated with the oxygen content, N:C, O:C, and H:C. Thus, as the distillation temperature increased, the oil compounds contained less heteroatoms, had an increased carbon content, yet also became more unsaturated. A lower oxygen content, acidity, fatty acid content, N:C, and O:C ratios led to a depressed energy content, whereas an increased content of saturated fatty acids, carbon, and hydrogen content augmented the energy content of the distillates. It's also interesting to note that the average weight of the compounds in the oil was positively correlated with the content of oxygen and nitrogen in the biocrude oil, indicating the presence of melanoidin derivatives, Maillard compound derivatives, and high molecular weight nitrogen- and oxygen-containing functional groups could have contributed to the high molecular weight of the oil [47]. Moreover, the polydispersity index was inversely correlated with the distillation temperature, indicating the homogeneous nature of the oil distilled at higher temperatures.

With respect to the oil physical properties, the acidity content of the biocrude oil was positively correlated with the oxygen, O:C, and fatty acid composition and inversely correlated with the carbon content, energy content, and the presence of saturated fatty acids, indicating that the total acid content was related directly to the presence of fatty acids. The density was also inversely proportional to the carbon and hydrogen content, indicating that the presence of heteroatoms and unsaturated compounds tended to increase the density of the biocrude oil. Moreover, the density was strongly correlated with the viscosity, indicating that a denser oil was also more resistant to flow. Finally, the viscosity was slightly correlated with the decrease in the hydrogen content, indicating that unsaturation resulted in a lesser flow resistance.

Regarding the CCI, a high-quality fuel was correlated to the carbon, hydrogen, energy, saturated hydrocarbon, and olefin content.

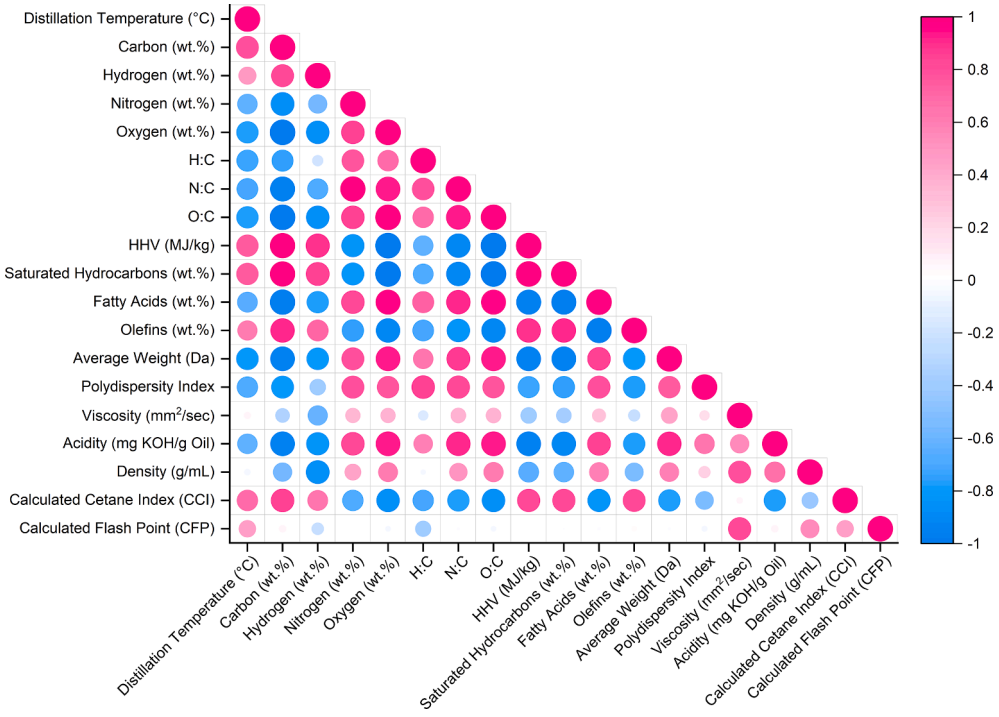

Fig. 8. Correlation between distillation response variables.

Furthermore, the presence of heteroatoms (oxygen, nitrogen, N:C, O:C, acidity, etc.) all contributed to a low CCI, indicating that a higher fractional distillation temperature favored the formation of a fuel with a higher CCI. CFP did not demonstrate a strong correlation with any of the other variables besides viscosity.

Fig. 9 synthesizes the data presented in this study and demonstrates the quantitative difference and blending potential between the light distillates (groups 1–6) and medium distillates (groups 7–14) relative to the three base fuels. A positive value signifies a value higher than the base fuel, and a negative value signifies a value lower than the base fuel. The blending percentages were defined as weight percentage of distillate to weight percentage base fuel. The blending areas were determined by taking the median value of the poorest fuel characteristic and assuming different blending ratios with the base fuel. Notably, some characteristics of the distillates only slightly deviated from the base fuels: H:C (-11.2–20.7%), HHV (-16.5–6.2%), density (-8.0–26.4%), polydispersity index (11.6–34.3%). However, many characteristics deviated from the base fuels by more than 100% compared to the base fuels: N:C (80.6–2,490.5%), viscosity (-28.4–756.5%), acidity (-100.0–1,573.4%), average molecular weight (15.7–103.4%), and CFP (-379.3–633.9%). Thus, supplanting conventional fuels with HTL-derived fuels is not feasible, and blending with the base fuel is necessary to ensure that the blended fuel retains properties similar to the base fuel. Most notably, the fractional distillates deviated least with Jet A, amounting to 10%, 25%, and 50% blending ratios that only deviated from Jet A by as much as ±63.3%, ±158.3%, and ±316.6%, respectively. Thus, distillates derived from the pilot-scale HTL of food waste demonstrate potential to form a Jet A blendstock. However, blends with gasoline were not as promising, amounting to deviations with the base fuel as high as ±214.7%, ±536.8%, and ±1,073.6% for a 10%, 25%, and 50% blend, respectively. Thus, additional processing is necessary to improve the physical and chemical characteristics to even achieve a blended fuel that is comparable to gasoline.

4. Conclusions

This study demonstrated that biocrude oil derived from the mobile, pilot-scale HTL conversion of food waste could be successfully distilled into light (groups 1–6) and medium (groups 7–14) distillate fractions at atmospheric pressure. Fractional distillation effectively separated the asphaltenes (boiling point > 300 °C), thereby augmenting the quality of the biocrude oil distillates. Results demonstrated that distillation resulted in fractions of biocrude oil that were chemically (H:C, HHV, average molecular weight), physically (density), and thermally (CCI, boiling point distribution) similar to gasoline, diesel, and Jet A fuel. However, even with significant blending, the N:C, viscosity, and acidity were still high. Blending with unconventional fuels holds promise to bolster the supply of transportation fuels. Specifically, blending of the distillates with Jet A between 10 and 50% was the most encouraging among the fuels, thereby demonstrating potential for the combined

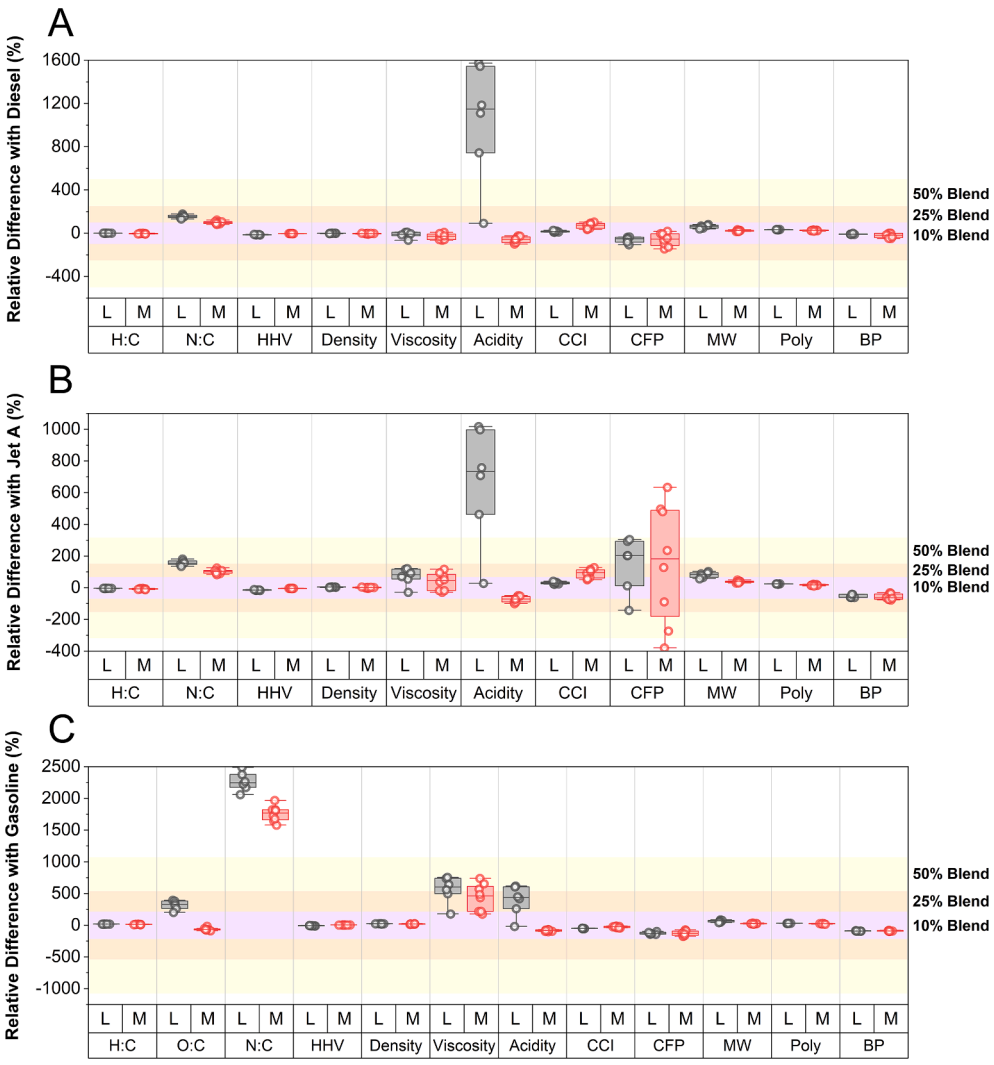

Fig. 9. Comparison of base fuels with biocrude oil distillates. L represents the light distillates (groups 1–6), and M represents the medium distillates (groups 7–14). HHV represents the higher heating value, CCI represents the calculated cetane index, CFP represents the calculated flash point, MW represents the average molecular weight, Poly represents the polydispersity index, and BP represents the 99% boiling point distribution. The 10%, 25%, and 50% blending regions were determined based on the median poorest characteristic of each fuel, and these regions signify that all characteristics would fall within this range upon blending.

pilot-scale HTL and fractional distillation process to be retrofitted with current petroleum technology. Blending with diesel and gasoline with the distillates in this study did not demonstrate as favorable of results. Additional thermocatalytic processing techniques (hydrotreating, hydrocracking) are needed to increase the blending ratio of distillates and further meet the standards and specifications of conventional fuels.

CRediT authorship contribution statement

Jamison Watson: Investigation, Methodology, Formal analysis, Visualization, Writing - original draft, Writing - review & editing. **Buchun Si:** Writing - review & editing, Investigation. **Zixin Wang:** Writing - review & editing, Investigation. **Tengfei Wang:** Investigation. **Amanda Valentine:** Writing - review & editing, Visualization. **Yuanhui Zhang:** Project administration, Supervision, Writing - review & editing.

Declaration of Competing Interest

The authors declare that they have no known competing financial interests or personal relationships that could have appeared to influence the work reported in this paper.

Acknowledgements

The authors acknowledge the financial support provided by the National Science Foundation US-China INFEWS grant (NSF# 18-04453 and 1744775) and the Jonathan Baldwin Turner Ph.D. Fellowship provided by the University of Illinois at Urbana-Champaign.

Compliance with Ethical Standards

The authors declare that they have no conflict of interest. All authors have read and have abided by the statement of ethical standards.

Appendix A. Supplementary data

Supplementary data to this article can be found online at https://doi.org/10.1016/j.fuel.2021.121028.

References

[1] US Environmental Protection Agency. Reducing Wasted Food At Home n.d. https://www.epa.gov/recycle/reducing-wasted-food-home.
[2] US Environmental Protection Agency. America's Food Waste Problem n.d.
[3] Kibler KM, Reinhart D, Hawkins C, Motlagh AM, Wright J. Food waste and the food-energy-water nexus: a review of food waste management alternatives. Waste Manag 2018;74:52–62. https://doi.org/10.1016/j.wasman.2018.01.014.
[4] Amini HR, Reinhart DR. Regional prediction of long-term landfill gas to energy potential. Waste Manag 2011;31(9-10):2020–6. https://doi.org/10.1016/j.wasman.2011.05.010.
[5] Pham TPT, Kaushik R, Parshetti GK, Mahmood R, Balasubramanian R. Food waste-to-energy conversion technologies: current status and future directions. Waste Manag 2015;38:399–408. https://doi.org/10.1016/j.wasman.2014.12.004.
[6] Dimitriadis A, Bezergianni S. Hydrothermal liquefaction of various biomass and waste feedstocks for biocrude production: a state of the art review. Renew Sustain Energy Rev 2017;68:113–25. https://doi.org/10.1016/j.rser.2016.09.120.
[7] Tian C, Li B, Liu Z, Zhang Y, Lu H. Hydrothermal liquefaction for algal biorefinery: a critical review. Renew Sustain Energy Rev 2014;38:933–50. https://doi.org/10.1016/j.rser.2014.07.030.
[8] Yu G, Zhang Y, Schideman L, Funk T, Wang Z. Distributions of carbon and nitrogen in the products from hydrothermal liquefaction of low-lipid microalgae. Energy Environ Sci 2011;4:4587–95. https://doi.org/10.1039/c1ee01541a.
[9] Chen W-H, Lin Y-Y, Liu H-C, Chen T-C, Hung C-H, Chen C-H, et al. A comprehensive analysis of food waste derived liquefaction bio-oil properties for industrial application. Appl Energy 2019;237:283–91. https://doi.org/10.1016/j.apenergy.2018.12.084.
[10] Xu F, Li Y, Ge X, Yang L, Li Y. Anaerobic digestion of food waste – Challenges and opportunities. Bioresour Technol 2018;247:1047–58. https://doi.org/10.1016/j.biortech.2017.09.020.
[11] Chen W-T, Zhang Y, Lee TH, Wu Z, Si B, Lee C-F, et al. Renewable diesel blendstocks produced by hydrothermal liquefaction of wet biowaste. Nat Sustain 2018;1(11):702–10. https://doi.org/10.1038/s41893-018-0172-3.
[12] Kassem N, Hockey J, Lopez C, Lardon L, Angenent LT, Tester JW. Integrating anaerobic digestion, hydrothermal liquefaction, and biomethanation within a power-to-gas framework for dairy waste management and grid decarbonization: A techno-economic assessment. Sustain Energy Fuels 2020;4(9):4644–61. https://doi.org/10.1039/D0SE00608D.
[13] Huq NA, Hafenstine GR, Huo X, Nguyen H, Tifft SM, Conklin DR, et al. Toward net-zero sustainable aviation fuel with wet waste–derived volatile fatty acids. Proc Natl Acad Sci 2021;118:e2023008118. doi: 10.1073/pnas.2023008118.
[14] Aierzhati A, Stablein MJ, Wu NE, Kuo C-T, Si B, Kang Xu, et al. Experimental and model enhancement of food waste hydrothermal liquefaction with combined effects of biochemical composition and reaction conditions. Bioresour Technol 2019;284:139–47. https://doi.org/10.1016/j.biortech.2019.03.076.
[15] Watson J, Wang T, Si B, Chen W-T, Aierzhati A, Zhang Y. Valorization of hydrothermal liquefaction aqueous phase: pathways towards commercial viability. Prog Energy Combust Sci 2020;77:100819. https://doi.org/10.1016/j.pecs.2019.100819.
[16] Pedersen TH, Jensen CU, Sandström L, Rosendahl LA. Full characterization of compounds obtained from fractional distillation and upgrading of a HTL biocrude. Appl Energy 2017;202:408–19. https://doi.org/10.1016/j.apenergy.2017.05.167.
[17] Hoffmann J, Jensen CU, Rosendahl LA. Co-processing potential of HTL bio-crude at petroleum refineries–Part 1: Fractional distillation and characterization. Fuel 2016;165:526–35.
[18] Taghipour A, Ramirez JA, Brown RJ, Rainey TJ. A review of fractional distillation to improve hydrothermal liquefaction biocrude characteristics; future outlook and prospects. Renew Sustain Energy Rev 2019;115:109355. https://doi.org/10.1016/j.rser.2019.109355.
[19] Ocfemia KS, Zhang Y, Funk T. Hydrothermal processing of swine manure into oil using a continuous reactor system: development and testing. Trans ASABE 2006;49:533–41.
[20] Aierzhati A, Watson J, Si B, Stablein M, Wang T, Zhang Y. Development of a mobile, pilot scale hydrothermal liquefaction reactor: food waste conversion product analysis and techno-economic assessment. Energy Convers Manag X 2021;10:100076. https://doi.org/10.1016/j.ecmx.2021.100076.
[21] Chen W, Wu Z, Si B, Zhang Y. Renewable Diesel Blendstocks and Biopriviliged Chemicals Distilled from Algal Biocrude Oil Converted via Hydrothermal Liquefaction n.d.:1–32.
[22] Lu J, Zhang J, Zhu Z, Zhang Y, Zhao Yu, Li R, et al. Simultaneous production of biocrude oil and recovery of nutrients and metals from human feces via hydrothermal liquefaction. Energy Convers Manag 2017;134:340–6. https://doi.org/10.1016/j.enconman.2016.12.052.
[23] Chen W-T, Zhang Y, Zhang J, Yu G, Schideman LC, Zhang P, et al. Hydrothermal liquefaction of mixed-culture algal biomass from wastewater treatment system into bio-crude oil. Bioresour Technol 2014;152:130–9. https://doi.org/10.1016/j.biortech.2013.10.111.
[24] ASTM Standard D4737-10: "Standard Test Method for Calculated Cetane Index by Four Variable Equation." ASTM Int 2016. doi: 10.1520/D4737-10R16.
[25] International A. ASTM Standard D7215-16: Standard Test Method for Calculated Flash Point from Simulated Distillation Analysis of Distillate Fuels 2008. doi: 10.1520/D7215-16.
[26] Álvarez A, Lapuerta M, Agudelo JR. Prediction of flash-point temperature of alcohol/biodiesel/diesel fuel blends. Ind Eng Chem Res 2019;58(16):6860–9. https://doi.org/10.1021/acs.iecr.9b0084310.1021/acs.iecr.9b00843.s001.
[27] International A. ASTM D974-12: Standard Test Method for Acid and Base Number by Color-Indicator Titration 2012. doi: 10.1520/D0974-12.
[28] ASTM International. ASTM Standard D446-12: "Standard Specifications and Operating Instructions for Glass Capillary Kinematic Viscometers" 2017. doi: 10.1520/D0446-12R17.
[29] Shakya R, Whelen J, Adhikari S, Mahadevan R, Neupane S. Effect of temperature and Na2CO3 catalyst on hydrothermal liquefaction of algae. Algal Res 2015;12:80–90. https://doi.org/10.1016/j.algal.2015.08.006.
[30] Mancio AA, da Mota SAP, Ferreira CC, Carvalho TUS, Neto OS, Zamian JR, et al. Separation and characterization of biofuels in the jet fuel and diesel fuel ranges by fractional distillation of organic liquid products. Fuel 2018;215:212–25. https://doi.org/10.1016/j.fuel.2017.11.029.
[31] Zheng J-L, Wei Q. Improving the quality of fast pyrolysis bio-oil by reduced pressure distillation. Biomass Bioenergy 2011;35(5):1804–10. https://doi.org/10.1016/j.biombioe.2011.01.006.
[32] Eboibi BEO, Lewis DM, Ashman PJ, Chinnasamy S. Hydrothermal liquefaction of microalgae for biocrude production: Improving the biocrude properties with vacuum distillation. Bioresour Technol 2014;174:212–21. https://doi.org/10.1016/j.biortech.2014.10.029.
[33] Cheng D, Wang L, Shahbazi A, Xiu S, Zhang B. Characterization of the physical and chemical properties of the distillate fractions of crude bio-oil produced by the glycerol-assisted liquefaction of swine manure. Fuel 2014;130:251–6. https://doi.org/10.1016/j.fuel.2014.04.022.
[34] Hu X, Wang Y, Mourant D, Gunawan R, Lievens C, Chaiwat W, et al. Polymerization on heating up of bio-oil: a model compound study. AIChE J 2013;59:888–900. https://doi.org/10.1002/aic.
[35] Chen W-T. Upgrading hydrothermal liquefaction biocrude oil from wet biowaste into transportation fuel. 2017.
[36] Haider M, Castello D, Michalski K, Pedersen T, Rosendahl L. Catalytic hydrotreatment of microalgae biocrude from continuous hydrothermal liquefaction: Heteroatom removal and their distribution in distillation cuts. Energies 2018;11(12):3360. https://doi.org/10.3390/en11123360.
[37] Speight J. Handbook of petroleum product analysis. vol. 53. 2nd ed. John Wiley & Sons, Inc.; 2015.

[38] Yanowitz J, Ratcliff MA, McCormick RL, Taylor J., Murphy MJ. Compendium of Experimental Cetane Numbers Compendium of Experimental Cetane Numbers. 2017.
[39] Demirbas A, Balubaid MA, Basahel AM, Ahmad W, Sheikh MH. Octane rating of gasoline and octane booster additives. Pet Sci Technol 2015;33(11):1190–7. https://doi.org/10.1080/10916466.2015.1050506.
[40] Gai C, Zhang Y, Chen W-T, Zhang P, Dong Y. An investigation of reaction pathways of hydrothermal liquefaction using Chlorella pyrenoidosa and Spirulina platensis. Energy Convers Manag 2015;96:330–9. https://doi.org/10.1016/j.enconman.2015.02.056.
[41] Han J, Li X, Kong S, Xian G, Li H, Li X, et al. Characterization of column chromatography separated bio-oil obtained from hydrothermal liquefaction of Spirulina. Fuel 2021;297:120695. https://doi.org/10.1016/j.fuel.2021.120695.
[42] Lu J, Liu Z, Zhang Y, Savage PE. Synergistic and antagonistic interactions during hydrothermal liquefaction of soybean oil, soy protein, cellulose, xylose, and lignin. ACS Sustain Chem Eng 2018;6(11):14501–9. https://doi.org/10.1021/acssuschemeng.8b0315610.1021/acssuschemeng.8b03156.s001.
[43] Zhang J, Shi Y, Cao H, Wu Y, Yang M. Conversion of palmitic acid to jet fuel components over Mo/H-ZSM-22 bi-functional catalysts with high carbon reservation. Appl Catal A Gen 2020;608:117847. https://doi.org/10.1016/j.apcata.2020.117847.
[44] Vozka P, Kilaz G. A review of aviation turbine fuel chemical composition-property relations. Fuel 2020;268:117391. https://doi.org/10.1016/j.fuel.2020.117391.
[45] Rannaveski R. Developing a Novel Method for Using Thermal Analysis to Determine Average Boiling Points of Narrow Boiling Range Continuous Mixtures. Tallinn University of Technology; 2018.
[46] Musthafa MM. Development of performance and emission characteristics on coated diesel engine fuelled by biodiesel with cetane number enhancing additive. Energy 2017;134:234–9. https://doi.org/10.1016/j.energy.2017.06.012.
[47] Watson J, Swoboda M, Aierzhati A, Wang T, Si B, Zhang Y. Biocrude oil from algal bloom microalgae: a novel integration of biological and thermochemical techniques. Environ Sci Technol 2021;55(3):1973–83. https://doi.org/10.1021/acs.est.0c0592410.1021/acs.est.0c05924.s001.